Original scientific paper

Informacije MIDEM
Journal of Microelectronics,
Electronic Components and Materials
Vol. 47, No. 2(2017), 129 – 137

Highly Efficient Photocatalytic Activity in the Visible Region of Hydrothermally Synthesized N-doped TiO_2

Maja Lešnik[1], Dejan Verhovšek[1], Nika Veronovski[1], Srđan Gatarić[1], Mihael Drofenik[2], Janez Kovač[3]

[1]Cinkarna Celje, d.d. Inc., Celje, Slovenia
[2]University of Maribor, Faculty of Chemistry and Chemical Engineering, Maribor, Slovenia
[3]Jozef Stefan Institute, Department of Surface Engineering and Optoelectronics, Ljubljana, Slovenia

Abstract: Nanocrystalline rutile titanium dioxide (TiO_2) samples doped with various amounts of nitrogen (N) atoms were prepared using a hydrothermal synthesis route and a polycrystalline TiO_2 precursor. The doped rutile nanocrystallites were analysed with transmission electron microscopy (TEM), X-ray photoelectron spectroscopy (XPS) and UV–Vis spectroscopy. The Kubelka–Munk band-gap calculation were used to examine the UV–Vis reflectance spectra. The measurements of the photocatalytic activity were performed utilizing FT-IR. A remarkable increase in the photocatalytic activity of the doped rutile nanocrystallites was detected, when applying the isopropanol degradation method with UV–Vis light irradiation.

Keywords: Nanoparticles, TiO_2, Rutile, Visible photocatalyst

Hidrotermalno sintentiziran TiO_2 dopiran z N z visoko fotokatalitsko aktivnostjo v vidnem delu svetlobnega spektra

Izvleček: Z uporabo hidrotermalne sinteze in polikristalinične rutilne oblike nanodelcev TiO_2 smo pripravili monokristalinične rutilne delce, dopirane z različnimi koncentracijami dopanta N. Za analizo dopiranih rutilnih TiO_2 nanodelcev smo uporabili elektronsko mikroskopijo (TEM), fotoelektronsko spektroskopijo (XPS), rentgensko praškovno difrakcijo (XRD), UV-VIS spektroskopijo in kalkulacijo energijskih vrzeli s Kubelka Munk. Pri merjenju fotokatalitske aktivnosti z metodo degradacije izporopanola v alkohol smo ugotovili, da dopiranje rutilnega TiO_2 z N povzroči izrazit premik delovanja fotokatalitske aktivnosti na vidni svetlobi svetlobnega spektra.

Ključne besede: Nanodelci, TiO_2, rutil, vidni fotokatalizator

** Corresponding Author's e-mail: maja.lesnik@cinkarna.si*

1 Introduction

Nanocrystalline titanium dioxide (TiO_2) is the most widely investigated n-type semiconductor due to its high photocatalytic activity under UV light, which is important for numerous outdoor applications, such as wastewater treatment, air purification and self-cleaning applications (walls, concretes). [1-8] Recently, new insights have been presented in the development of TiO_2 photocatalysts that could efficiently utilize not only the UV light but also the visible light in the solar spectrum and could therefore be appropriate for interior photochemical applications. [8-16] Chemical modifications of the TiO_2 crystal lattice achieved by doping with cations or anions appear to be the most promising approach to enhance the visible-light absorption power. [17]

The dopants can be interstitially or substitutionally incorporated into the TiO_2 crystal lattice. Different concentration levels of these dopants might influence the new electronic states localized in the gap or the electronic band edge narrowing, leading to an increase in the visible-light absorption efficiency. [14, 17] However, it is well known that the photocatalytic activity under exposure to visible light, associated with the mobility of the excited electrons and holes and their recombination rate, differs, depending on the dopant type, its concentration and the lattice position that it occupies. [14, 17] On the other hand, anion doping has a tremendous effect on visible-light photocatalytically active TiO_2. [18, 19] Among all the attempts at non-metal doping in TiO_2, nitrogen doping has shown the greatest promise for achieving visible-light active photocatalysts. The incorporation of nitrogen into the TiO_2 crystal lattice is advantageous, due to it having a similar atomic radius to oxygen and a lower electronegativity than oxygen. [20] The modification mechanism of N-doped TiO_2, its ability to absorb visible light and visible-light photocatalysis is still under investigation. There are three different hypotheses that could explain the phenomena. Firstly, in N-doped TiO_2 the energies of the N 2p and O 2p states are similar. The consequence of this is band-gap narrowing and the ability to absorb visible light. [22] Secondly, oxygen sites are substituted by nitrogen atoms and the intermediate energy level is formed below the conductive band edge. [21] Thirdly, doping with nitrogen forms oxygen-vacancy defect sites, which are the major factor in visible-light photocatalytic activity. [23, 24] Rutile, as an n-type TiO_2 semiconductor, exhibits oxygen vacancies on the surface. Nitrogen doping introduces additional oxygen vacancies, which leads to an even more efficient photocatalytic activity. [25]

It is well known that the absorption properties of N-doped anatase and raw rutile TiO_2 are distinguishable. The structures of anatase and rutile differ in the position of the octahedron, resulting in a tetragonal structure for both modifications. [3] The other reason for the different absorption is the electron density of the N-doped anatase or rutile. [26] Doping with nitrogen provides N 2p states located above the O 2p valence band. Since rutile has a smaller band gap than anatase, this furthermore enhances the valence band. [27] The same findings were confirmed by Yang and co-authors in their DFT calculations on nitrogen-doped structures of rutile crystals. [15] Liu, in his work, demonstrated that nitrogen-doped TiO_2 with more rutile phase has more defects than the nitrogen-doped TiO_2 with less rutile phase, which enhances the photocatalytic efficiency. [25] The photocatalytic efficiencies of rutile and anatase are related to the formation of hydroxyl radicals that prevent electron–hole recombination during exposure to sunlight. Some studies have demonstrated that the rutile crystal phase exhibits enough hydroxyl groups, which are believed to act as light photocatalysts, i.e., to accept the holes generated by UV illumination and form hydroxyl radicals and thus prevent electron–hole recombination. [28, 29]

The selection of nitrogen doping for the rutile crystal structure was based on theoretical studies published recently in the open literature, particularly on the numerous advantages of visible-light absorption and enhanced photocatalytic activity. [26-29]

In the present study we report a new synthesis procedure of N-TiO_2 visible-light photocatalyst based on the hydrothermal synthesis using the polycrystalline rutile TiO_2 nanocrystallites.

2 Experimental

2.1 Preparation method

The hydrothermal synthesis of N-doped rutile TiO_2 nanocrystallites was performed in a Teflon-lined, stainless-steel autoclave with a volume of 80 mL. To prepare the TiO_2-doped sample the reactor was loaded with a 50-mL aqueous suspension of polycrystalline rutile TiO_2 nanocrystallites provided by Cinkarna Celje, Inc., having a mass concentration between 60-150 g/L (calculated as TiO_2) and 1 mass % (based on TiO_2 content) of urea ($(NH_2)_2CO$, 99% w/w, Merck). The mixture of polycrystalline rutile TiO_2 nanocrystallites and dopant was then stirred for at least 15 minutes. The autoclave was put into a preheated oven and was hydrothermal treated at 180 °C for 24 hours. At the end of the heating process the autoclave was taken out of the oven and left to cool to room temperature. The as-prepared product was diluted with distilled water, washed on a laboratory centrifuge (MPW 350 – Med. Instruments, High brushless centrifuge, 4000 rpm, 20 minutes). The washing was continued until the conductivity of the effluent was less than 900 µS/cm. The final product was an aqueous suspension of doped rutile having 10 mass % of TiO_2 nanocrystallites. Samples with urea/TiO_2 ratios of 0.01, 0.02, 0.03, 0.06, 0.08 w/w, labelled as samples: *B, C* and *D*, *E, F*, were then prepared using the same process by varying the content of added urea. The sample *A* was prepared using the same process, but without the addition of urea as a dopant.

2.2 Characterization of samples

The crystallinity of the particles was examined using X-ray diffraction (XRD) performed on a Cubi X PRO PW

3800 instrument (PANanalytical) (Cu-Kα radiation (λ = 1.5418Å)). In order to acquire the TiO_2 powders for the X-ray powder-diffraction (XRD) measurement, the suspensions were dried at 80 °C, ground and the powder pressed into pellets that were used to perform the measurements.

The average crystallite size was determined using diffraction-peak (100) broadening and Scherrer's formula based on the FWHM (Full Width at Half Maximum) of the XRD peak.

The specific surface areas (S_{BET}) of particles were determined using Tristar 3000, the automatic gas analyser (Micromeritics Instrument Co.).

The morphology and the size of the particles were examined with a transmission electron microscope (TEM, Jeol JEM-2100, Jeol Ltd.,Tokyo, Japan). The samples for the TEM specimens were ultrasonically dispersed and the suspensions were collected using carbon-supported copper grids.

The UV–Vis diffuse reflectance spectra were collected on an Agilent-Cary 300 UV–Vis spectrophotometer equipped with an integrating sphere (Varian Inc., USA).

The measurements of the photocatalytic activity were performed in a sealed gas-solid reactor at room temperature and a relative humidity of 60%, utilizing FT-IR spectroscopy (Spectrum BX model Perkin Elmer spectrometer). The model pollutant was isopropanol in the gas phase. During the photocatalytic reaction the isopropanol oxidizes to acetone and subsequently to carbon dioxide and water under UV irradiation (Xe lamp, 300 W). The light imitates the solar spectrum and emits both ultraviolet (UV) and visible (VIS) light. The reactor is at a distance of 4 cm from the lamp. The samples were dried under ambient conditions and prepared by milling 50 mg of the material. To perform the measurements, 20 µL of isopropanol was injected into the system. This volume represents around 2000 ppm of gas phase for the isopropanol in the system. The amount and ratio of isopropanol and the formed acetone were monitored in real time. The evaluation of the photocatalytic activity is based on the acetone-formation kinetics and is given in ppm/h. [33]

The chemical composition of the surfaces was determined by X-ray photoelectron spectroscopy (XPS). XPS analyses were performed with a TFA XPS spectrometer, produced by Physical Electronics Inc., equipped with a monochromated Al–K_α X-ray source (1486.6 eV), under ultra-high vacuum (10^{-7} Pa). Samples in the form of powders were deposited on the adhesive carbon tape. The analyzed area was 0.4 mm in diameter and the analyzed depth was 3–5 nm. The high-energy resolution spectra were acquired with an energy analyzer operating at a resolution of about 0.6 eV and a pass energy of 29 eV. The XPS spectra were processed with the software MultiPak. Prior to the spectra processing, the same spectra were referenced to the C-C/C-H peak in the C 1s core level at a binding energy of 284.8 eV. The accuracy of the binding energies was about ± 0.2 eV. Quantification of the surface composition was based on the XPS peak intensities, taking into account the relative sensitivity factors provided by the instrument manufacturer. [38] Three different places were analyzed on each sample and the data were averaged.

3 Results and discussion

3.1 The crystallite phase and size of rutile particles

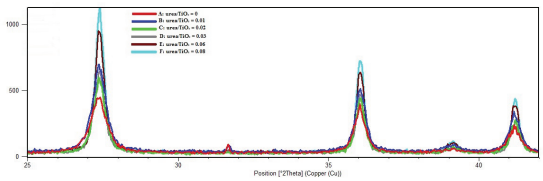

Figure 1: XRD patterns of undoped and N-doped TiO_2 samples with different ratios of urea to TiO_2.

Figure 1 presents the XRD patterns of the samples prepared using a modified hydrothermal process and various ratios of urea to TiO_2. The presence of specific peaks (2θ = 27.38°, 36.06°, 41.19°) was taken as an attributive indicator of rutile titania. [20, 31] However, no N-derived peak is detected for N-TiO_2, even when the ratio of urea to TiO_2 was 0.08. It can also be seen from the XRD patterns that the nitrogen-doped samples show more intensive diffraction peaks, indicating a more pronounced crystallinity for the N-doped crystallites.

From Table 1 it is clear that the crystallite size increases with the amount of urea in the precursor suspension, i.e., the ratio of urea to polycrystalline TiO_2 (w/w) precursor changes from 0.01 to 0.08. The increase of the crystallite size, for identical hydrothermal conditions, due to a larger amount of urea, can be assigned to the vigorous thermally assisted decomposition reaction of the urea, which enhances the kinetics of mass transport during the dissolution, precipitation and growth of TiO_2 nano-crystallites. Thus, a crystallite-size increase is straightforward and proportional to the amount of urea in the starting suspension. On the other hand, when the addition is a compound that is stable during the hydrothermal synthesis conditions it would, as expected, hinder the crystallite growth and thus decrease

the final crystallite size, which is the case when the suppression of crystallites size is planned.

As a consequence, the specific surface areas (S_{BET}) show a steady decrease in parallel with the crystallite size increase. Here, an exception proves sample *B* with a much smaller specific surface regarding the general trend in the sequence, which might be a consequence of the exaggerated crystallite agglomeration. However, in general the morphology of the crystallites follows the general expectation.

Table 1: Average crystallite size, specific surface area and band-gap energies for various N-doped TiO_2 samples.

Sample	Urea/TiO_2	Specific surface area (m^2/g)	Crystallite size (100) (nm)	Band gap (eV)
A	-	70.1	16.7	3.01
B	0.01	42.5	23.6	3.04
C	0.02	68.1	27.6	3.03
D	0.03	63.7	33.0	3.03
E	0.06	56.9	42.6	3.04
F	0.08	51.0	48.7	3.02

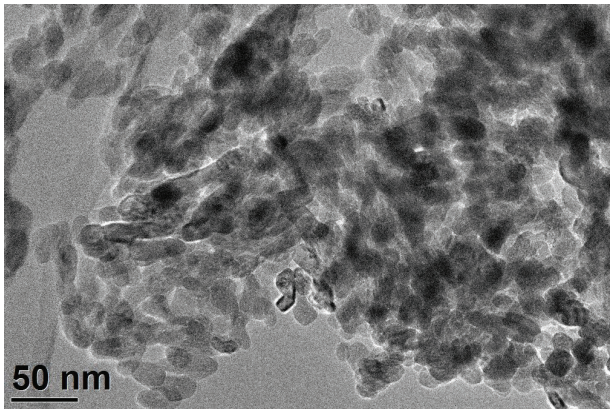

(a)

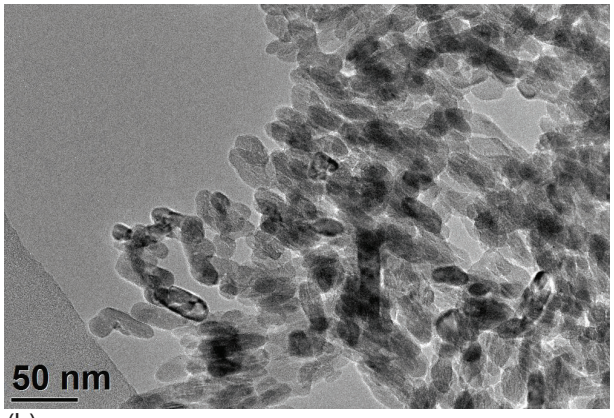

(b)

Figure 2: TEM micrographs of samples prepared with different ratios of urea to TiO_2: (a) undoped TiO_2 and (b) urea/TiO_2 = 0.02.

3.2 The morphology of the doped TiO_2 particles

The morphologies of the N-doped TiO_2 are shown in the TEM micrographs of Figure 2. The hydrothermally synthesized, doped, rutile TiO_2 nanocrystallites have an oval/spherical morphology and are uniform in size. The crystallite sizes observed with the TEM match with those obtained from the Scherrer estimation using the peak broadening of the XRD spectra, which has shown a comparable crystallite size up to a urea/TiO_2 ratio of 0.03.

On the other hand, the morphologies of samples E and F, prepared at ratios of urea to TiO_2 of 0.06 and 0.08, respectively, exhibit a larger crystallite size (TEM images not shown).

3.3 UV–Vis diffuse reflectance spectra

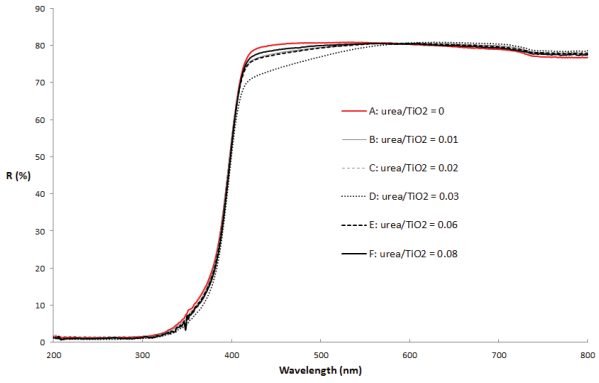

Figure 3: UV–Vis reflectance spectra of the undoped TiO_2 and the TiO_2 doped with different urea-to-TiO_2 ratios, indicated in the legend.

For the examination of the effects of doping on TiO_2, an evaluation of the optical properties is the most appropriate method. UV–Vis spectroscopy and diffuse reflectance spectroscopy were chosen as the techniques for the optical studies of N-doped TiO_2. In our work diffuse reflectance spectroscopy was used to examine the visible-light sensitivity. The influence of nitrogen doping on the UV–Vis spectra properties for the rutile TiO_2 is demonstrated in Figure 3. The reflectivity dependence of the wavelength of the pure TiO_2 has a typical sharp edge of reflection at around 420–400 nm. Compared with the spectrum of undoped TiO_2, the N-doped sam-

ples exhibit a very similar curve progression; however, there is a small but distinguishable shift in the absorbance region of the visible range 400–550 nm. [30, 31, 34] The N-doped samples exhibit a slightly difference in the colour, which could provide a small absorbance in visible region. [41] An exception is observed for the 0.03-doped sample *D*, which shows a more notable red shift. So, based on the intensity of absorption for all the samples we can assume that the nitrogen entered the TiO_2 crystal lattice under the reported hydrothermal condition. The same finding was reported by Huang. [31]

It was reported that the visible-light absorption could be brought about by band-gap narrowing. However, it was also reported that the localized N states within the band gap and the Ti^{3+} defects could also provide the absorption red shift. [34, 35] In addition, Hu showed that the band gaps of the doped samples were the same, indicating that N doping did not change the band gap of the TiO_2. [32] The doping of TiO_2 with N atoms improved its visible-light absorption, increased the numbers of photons in the photocatalytic reaction and thus enhanced the photocatalytic activity in the visible region.

The band-gap energies of the rutile nanocrystallites, estimated using Kubelka–Munk model are summarised in Table 1. [35, 36] The values of the band-gap energies of the doped samples were compared with a control sample (undoped rutile nanocrystallites), which was calculated to have a band gap of 3.01 eV. The calculated value for the undoped rutile nanocrystallites is in agreement with the theoretical value of 3.0 eV for the rutile modification. [37] The results show that the band-gap energies of all the N-doped samples are practically the same as the control sample. A possible explanation is that the visible-light absorption occurs due to the colour centres formed by the N-doping process rather than by a narrowing of the band gap. The research was conducted on various N-doped metal-oxide nanoparticles. The band-gap narrowing does not occur, even for significantly high doping levels, such as 25 % doping. [32, 34]. It can be concluded that the main effect of N doping is a slightly improved absorption at long wavelengths, which enhances the visible photocatalytic activity of these material. It could be concluded that the main effect of N doping is the improved absorption at long wavelengths due to the shallow trap states inside the TiO_2 crystal lattice, which enhances the visible photocatalytic activity of these materials. [22, 24, 25]

3.4 Investigation of chemical states of TiO_2 samples

The surface chemical composition and the chemical states of the TiO_2 samples were analyzed by means of XPS. The survey spectra (not shown) are similar and indicate the presence of Ti, O and C in all the samples, while N is visible only in the spectra from the urea-modified TiO_2 samples and confirms a successful treatment. The surface chemical compositions are presented in Table 2. The carbon on the surface of the undoped sample can be related to the surface contamination and the synthesis conditions. For the TiO_2 samples treated with urea a nitrogen signal appeared. The highest nitrogen concentration (0.8 at.%) was observed on the surface of the TiO_2 sample D (urea/TiO_2 ratio 0.03). On the sample treated with a higher urea concentration, sample F (urea/TiO_2 ratio 0.08), we observed less nitrogen (~ 0.3 at.%). The amount of nitrogen on the surfaces of the analyzed samples correlates with the photocatalytic activity.

High-energy-resolution C 1s, O 1s, N 1s and Ti 2p XPS spectra were acquired to further understand the chemical bonding. In the high-energy-resolution O 1s spectra (not shown here) we were able to observe the presence of two different components by using a fitting procedure. The main contribution is attributed to the Ti-O in the TiO_2 (529.9 eV) and the other minor peak can be ascribed to the surface hydroxyl Ti-OH (531.4 eV). [39] A comparison of the O 1s spectra from the undoped sample with the treated samples shows no major differences.

Nitrogen was only detected in the urea-treated TiO_2 samples. High-energy-resolution N 1s XPS spectra from the undoped TiO_2 and the TiO_2/urea ratio of 0.03 are shown on Figure 4. The maxima of the N 1s spectra, for all the treated samples, are located at 400 eV, which indicates interstitial nitrogen integrated into the TiO_2 lattice. It is known that the peak at around 400 eV is related to the N-O, N-C or N-N type of bonds. [40]

A comparison of the high-energy-resolution Ti 2p spectra from all the analysed samples is shown in Figure 5. In the acquired Ti 2p spectra a doublet peak is visible, containing both Ti $2p_{3/2}$ and Ti $2p_{1/2}$ components, which appear at 458.6 eV and 464.3 eV, respectively, with 5.7 eV spin-orbital splitting. This corresponds to a Ti^{4+} va-

Table 2: Surface composition in at. % of the undoped TiO_2 and TiO_2 modified with urea using different concentrations.

Sample	Urea/TiO_2	C	O	Ti	N
A	-	26.1	52.2	21.7	
B	0.01	21.5	55.8	22.3	0.3
C	0.02	23.4	54.6	21.4	0.7
D	0.03	24.8	53.4	21.1	0.8
E	0.06	20.0	56.7	22.7	0.6
F	0.08	25.2	53.1	21.4	0.3

lence state. The peaks are narrow and no significant differences, like shifting in the binding energy, between the undoped and treated samples were observed (Figure 5).

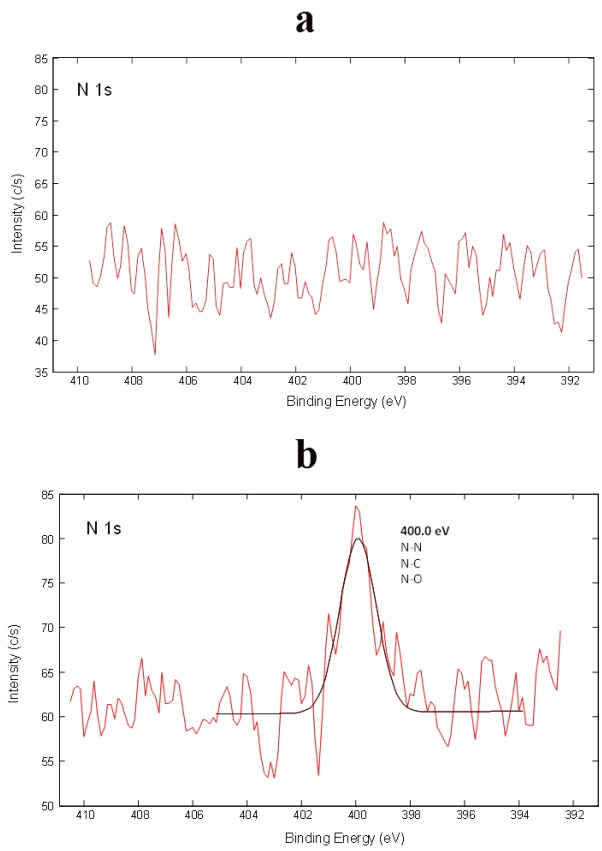

Figure 4: N 1s XPS spectrum of undoped TiO_2 (a) and TiO_2 modified with a TiO_2/urea ratio = 0.03 (b).

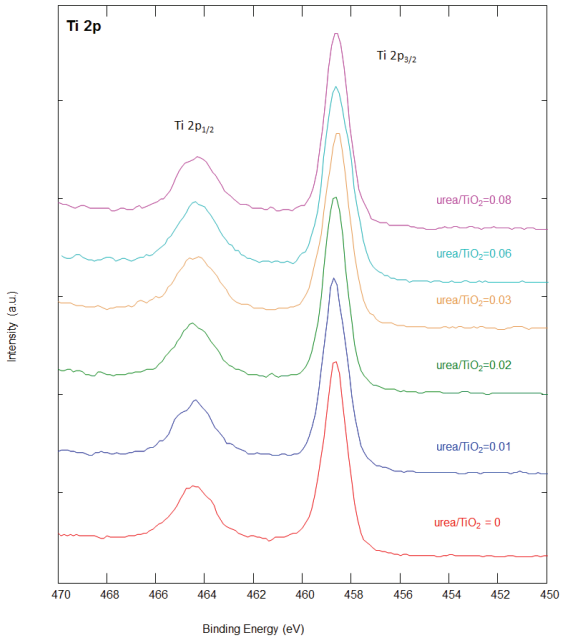

Figure 5: XPS spectra of Ti 2p from all the samples.

3.5 Photocatalytic activity measurements

To evaluate the photocatalytic activity of the undoped and N-doped TiO_2 in the visible range, the degradation of isopropanol under UV+VIS and Vis irradiation was investigated. The results of the photocatalytic activities are presented in Figure 6, based on the acetone-formation kinetics, and are given in ppm/h. As illustrated in Figure 6, different N-doped TiO_2 catalysts differ in the degradation of isopropanol under the same experimental conditions. One can see that i) in general, N-doped TiO_2 samples achieve a higher photocatalytic activity than the undoped TiO_2 samples and ii) the photocatalytic activity increases with the surface-nitrogen concentration.

Among all of the investigated N-doped TiO_2 samples, sample *E*, with a urea/TiO_2 ratio of 0.06 and a corresponding surface-nitrogen concentration of 0.6 at %, displays the highest photocatalytic efficiency for isopropanol degradation. Nearly the same photocatalytic efficiency was also detected with the sample C, having otherwise a lower urea/TiO_2 ratio of 0.02; however, it exhibits a similar surface-nitrogen concentration of 0.7 at %. In addition, sample E exhibits a lower specific surface area than the sample C with a urea/TiO_2 ratio of

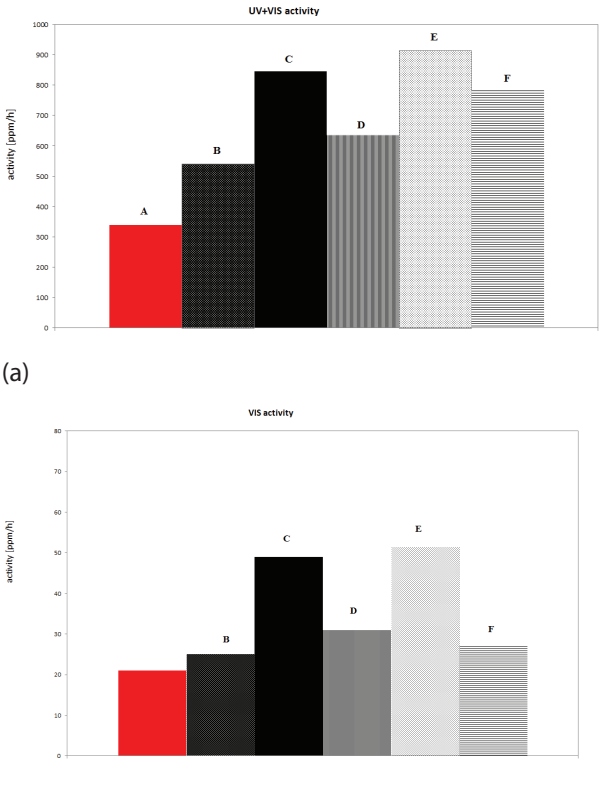

Figure 6: Photocatalytic activity of undoped TiO_2 and TiO_2 doped with different ratios of urea under a) UV+Vis irradiation and b) Vis irradiation.

0.02, Table 1. Therefore, the high photocatalytic activity of sample *C* with a surface nitrogen concentration of 0.7 at % is not a consequence of a higher specific surface area, but the result of a high surface-nitrogen concentration. This is in accordance with the general trend that the $N^{\cdot}$ centres enhanced the photocatalytic activity in the visible range.

As a result, an increase in the surface area does not automatically produce an increase in the photocatalytic activity, demonstrating that the higher activity is a consequence of a high surface-nitrogen concentration and not of the surface-regulated process. On the other hand, a greater surface area provides more active sites on the TiO_2 surface for the degradation of the organic pollutant. [20, 32]

4 Conclusions

N-doped rutile TiO_2 nanocrystallites that exhibit a strong increase in their photocatalytic activity were successfully prepared using the hydrothermal method. The absorbance of N-TiO_2 in the visible-light region is the most important when concerning the material's application since it can be activated with solar light and thus exhibits an enhanced photocatalytic visible-light activity. The narrowing of the band gap does not occur, indicating that the major effects of N doping are an enhanced absorption at long wavelengths and the hole-trapping sites, which retards the hole–electron recombination and might be useful in enhancing the visible photocatalytic activity of these materials. The maxima of the N 1s spectra, for all the treated samples, indicate that the interstitial nitrogen is integrated into the TiO_2 lattice. The N-doped TiO_2 samples achieved a higher photocatalytic activity in the UV and visible-light regions than the undoped sample. This higher photocatalytic activity has a close correlation with the enhanced visible-light absorption of the doped samples.

5 Acknowledgment

This work is partially financially supported by the Ministry of Education, Science and Sport of the Republic of Slovenia under the contract 34/2013-SOF. The authors declare that there is no conflict of interest regarding the publication of this paper.

6 References

1. M. R. Hoffmann, S. T. Martin, W. Choi, D. W. Bahnemann, Environmental applications of semiconductor photocatalysis, Chem. Rev., 1995, 95(1), 69-96
2. A. Fujishima, T. N. Rao, D. A. Tryk, Titanium dioxide photocatalysis, Journal of Photochemistry and Photobiology C: Photochemistry, 2000, 1, 1-21
3. M. Palaez, N. T. Nolan, S. C. Pillai, M. K. Seery, P. Falaras, A. G. Kontos, P. S. M. Dunlop, J. W. J. Hamilton, J. A. Byrne, K. O'Shea, M. H. Entezari, D. D. Dionysiou, A review on the visible light active titanium dioxide photocatalysts for environmental applications, Applied Catalysts B: Environmental, 2012, 125, 331-349
4. X. Chen, S. S. Mao, Titanium dioxide nanomaterials: synthesis, properties, modifications and applications, Chem. Rev., 2007, 107, 2891-2959
5. D. P. Macwan, P. N. Dave, S. Chatuverdi, A review on nano-TiO_2 sol gel synthesis and its applications, J. Mater. Science, 2011, 46, 3669-3686
6. S. Banerjee, D. D. Dionysiou, S. C. Pillai, Self-cleaning applications of TiO_2 by photo-induced hydrophilicity and photocatalysis, Applied Catalysis B: Environmental, 2015, 176-177, 396-428
7. W. Shen, C. Zhang, Q. Li, W. Zhang, L. Cao, J. Ye, Preparation of titanium dioxide nano particle modified photo catalytic self-cleaning concrete, Journal of cleaner production, 2015, 87, 762-765
8. S. M. Gupta, M. Tripathi, A review of TiO_2 nanoparticles, Chinese Science Bulletin, 2011, 56 (16), 1639-1657
9. S. Banerjee, S. C. Pillai, P. Falaras, K. E. O'Shea, J. A. Byrne, D. D. Dionysiou, New insights into the mechanism of visible light photocatalysis, The Journal of Physical Chemistry Letters, 2014, 5, 2543-2554
10. H. Feng, M. Zhang, L. E Yu, Hydrothermal synthesis and photocatalytic performance of metal-ions doped TiO_2, Applied Catalysis A: General, 2012, 413-414, 238-244
11. G. Liu, L. Wang, H. Gui Hang, H.-M. Cheng, G. Q. Lu, Titania-based photocatalysts-crystal growth, doping and heterostructuring, Journal of Materials Chemistry, 2010, 20, 831-843
12. A. Zaleska, Doped-TiO_2: A review, Recent Patents on Engineering, 2008, 2, 157-164
13. S. G. Kumar, L. G. Devi, Review on modified TiO_2 photocatalysis under UV/visible light selected results and related mechanisms on interfacial charge carrier transfer dynamics, The Journal of Physical Chemistry A, 2011, 115, 13211-13241
14. M. V. Dozzi, E. Selli, Doping TiO_2 with p-block elements: Effects on photo catalytic activity, Journal

of Photochemistry and Photobiology C: Photochemistry, 2013, 14, 13-28
15. Y. Dai, K. Yang, B. Huang, S. Han, Theoretical study of N-doped TiO_2 rutile crystals, J. Phys, Chem B, 2006, 110, 24011-24014
16. S. Rehman, R. Ullah, A. M. Butt, N.D. Gohar, Strategies of making TiO_2 and ZnO visible light active, Journal of Hazardous Materials, 2009, 170, 560-569
17. M. Fernandez-Garcia, A. Martinez-Arias, J. C. Conesa, Visible light – responsive titanium oxide photocatalysts: preparation based on chemical method, Environmentally Benign Photocatalysts, Nanostructure Science and Technology, 2010
18. C. Burda, Y. Lou, X. Chen, A. C. S. Samia, J. Stout, J. L. Gole, Enhanced nitrogen doping in TiO_2 nanoparticles, Nano Letters, 2003, 3 (8), 1049-1051
19. M. Long, W. Cai, Visible light responsive TiO_2 modification with non-metal elements, Frontiers of Chemistry in China, 2011, DOI 10.1007/s11458-011-0243-8
20. J. Ananpattarachai, P. Kajitvichyanukul, S. Seraphin, Visible light absorption ability and photo to catalytic oxidation activity of various interstitial N-doped TiO_2 prepared from different nitrogen dopants, Journal of Hazardous Materials, 2009, 168, 253-261
21. Z. L. Zeng, First principle study on the structural and electronic properties of N atoms doped rutile TiO_2 of oxygen vacancies, Advances in Materials Science and Engineering, 2014, 2015, 10 pages
22. M. Batzill, E. H. Morales, U. Diebold, Influence of nitrogen doping on the defect formation and surface properties of TiO_2 rutile and anatase, Physical Review Letters, 2006, 96 (2), 026103 (4)
23. B. Ohtani, Titania photocatalysis beyond recombination: A critical review, Catalysts, 2013, 3, 942-953
24. T. Ihara, M. Miyoshi, Y. Iriyama, O. Matsumoto, S. Sugihara, Visible light active titanium dioxide photocatalyst realized by an oxygen-deficient structure and by nitrogen doping, Applied Catalysis B: Environmental, 2003, 42, 403-409
25. G. Liu, X. Wang, Z. Chen, H. M. Cheng, G. Q. Lu, The role of crystal phase in determining photo catalytic activity of nitrogen doped TiO_2, Journal of Colloid and Interface Surface, 2009, 329, 331-338
26. C. Di Valentin, G. Pacchioni, A. Selloni, Origin of the different photocatalytic activity of N-doped anatase and rutile TiO_2, Physical review B, 2004, 70, 085116
27. O. Diwald, T. L. Thompson, E. G. Goralski, S. D. Walck, J. T. Yates, Jr., The effect of nitrogen ion implantation on the photo catalytic activity of TiO_2 rutile single crystals, J. Phys. Chem B, 2004, 108, 52-57
28. J. Lin, J. C. Yu, D. Lo, S. K. Lam, Photo catalytic activity of rutile $Ti_{1-x}Sn_xO_2$ solid solutions, Journal of Catalysis, 1999, 183, 368-372
29. H. Liu, L. Gao, Codoped rutile TiO_2 as a new photocatalyst for visible light irradiation, Chemistry Letters, 2004, 33 (6), 730-731
30. F. Peng, L. Cai, L. Huang, H. Yu, H. Wang, Preparation of nitrogen-doped titanium dioxide with visible light photo catalytic activity using a facile hydrothermal method, Journal of Physics and Chemistry of Solids, 2008, 69, 1657-1664
31. D. Huang, S. Liao, S. Quan. L. Liu, Z. He, J. Wan, W. Zhou, Synthesis and characterization of visible light responsive N-TiO_2 mixed crystal by a modified hydrothermal process, Journal of Non-Crystalline Solids, 2008, 354, 3965-3975
32. S. Hu, A. Wang, X. Li, H. Löwe, Hydrothermal synthesis of well-dispersed ultrafine N-doped TiO_2 nanoparticles with enhanced photo catalytic activity under visible light, Journal of Physics and Chemistry of Solids, 2010, 71, 156-162
33. M. Tashibi, U. Lavrenčič Štangar, A. Sever Škapin, A. Ristić, V. Kaučič, N. Novak Tušar, Titania-containing mesoporous silica powders: Structural properties and photocatalytic activity towards isopropanol degradation, Journal of Photochemistry and photobiology A: Chemistry, 2010, 216, 167-178
34. X. Qiu, C. Burda, Chemically synthesized nitrogen doped metal oxide nanoparticles, Chemical Physics, 2007, 339, 1-10
35. M. D'Arienzo, R. Scotti, L. Wahba, C. Battocchio, E. Bemporad, A. Nale, F. Morazzoni, Hydrothermal N-doped TiO_2: Explaining photo catalytic properties by electronic and magnetic identification of N active sites, Applied Catalysis B: Environmental, 2009, 93, 149-155
36. S. Valencia, J.M. Marin, G. Restrepo, Study of the bandgap of synthesized titanium dioxide nanoparticles using the sol-gel method and a hydrothermal treatment, The Open Materials Science, 2010, 4, 9-14
37. M. Landmann, E. Rauls, W.S. Schmidt, The electronic structure and optical response of rutile, anatase and brookite TiO_2, *J. Phys.: Condens. Matter, 2012,* 24 195503
38. J. F. Moulder, W. F. Stickle, P. E. Sobol, K. D. Bomben, "Handbook of X-Ray Photoelectron Spectroscopy", Physical Electronics Inc., Eden Prairie, Minnesota, USA, 1995
39. J. Yu, H. Yu, B. Cheng, M. Zhou, X. Zhao, Enhanced photocatalytic activity of TiO_2 powder (P 25) by hydrothermal treatment, Journal of Molecular Catalysis A:Chemical, 2006, 253, 112-118
40. Y. Nosaka, M. Matsushita, J. Nishino, A. Y. Nosaka, Nitrogen doped titanium dioxide photocatalysts

for visible response prepared by using organic compounds, Science and Technology of Advanced Materials, 2005, 6, 143-148.
41. P. He, J. Tao, X. Hunag, J. Xue, Preparation and photocatalytic antibacterial property of nitrogen doped TiO_2 nanoparticles, Sol-Gel Sci. Technol. 2013, 68, 213-218

Arrived: 23. 05. 2017
Accepted: 01. 08. 2017